Available online at www.sciencedirect.com

SciVerse ScienceDirect

Mathematics and Computers in Simulation 82 (2012) 1278–1286

MATHEMATICS AND COMPUTERS IN SIMULATION

www.elsevier.com/locate/matcom

Original article

A particle method for a collisionless plasma with infinite mass

Stephen Pankavich

Department of Mathematics, United States Naval Academy, Annapolis, MD 21402, United States

Received 16 September 2009; received in revised form 18 August 2011; accepted 31 August 2011
Available online 19 September 2011

Abstract

The one-dimensional Vlasov–Poisson system is considered and a particle method is developed to approximate solutions without compact support which tend to a fixed background of charge as $|x| \to \infty$. Such a system of equations can be used to model kinetic phenomena occurring in plasma physics. A localized particle method is constructed and implemented using the fact that solutions to the Vlasov–Poisson system propagate at finite speeds. Finally, the numerical method is utilized to ascertain information regarding the time asymptotics of the generated electrostatic field.

Keywords: Plasma; Particle method; Vlasov–Poisson; Infinite mass

1. Introduction

The motion of a collisionless plasma – an ionized gas of high-temperature and low-density – is described by the Vlasov–Maxwell system. If this fundamental kinetic model is posed in a two-dimensional phase space (one for spatial variables and another representing momentum) then Maxwell's equations simplify greatly and the problem reduces to the one-dimensional Vlasov–Poisson system. We consider this system of PDEs for the motion of negative charges upon prescribing a fixed, spatially-homogeneous background of positive ions:

$$\left.\begin{aligned} \partial_t f + v\partial_x f - E\partial_v f &= 0, \\ \partial_x E(t,x) &= \int (F(v) - f(t,x,v))dv \\ f(0,x,v) &= f_0(x,v). \end{aligned}\right\} \tag{1}$$

Here, $t \geq 0$ denotes time, $x \in \mathbb{R}$ is position, $v \in \mathbb{R}$ is momentum, $f(t,x,v)$ represents the density of negative ions or electrons, $F(v) \not\equiv 0$ is a given function describing the fixed background of positive charge, and $E(t,x)$ represents the electric field generated by the charges. We define

$$\rho(t,x) := \int (F(v) - f(t,x,v))dv$$

E-mail address: pankavic@usna.edu

0378-4754/$36.00
doi:10.1016/j.matcom.2011.08.007

to be the density of charge in the system. Throughout the present study, we will assume neutrality of the system

$$\int\int (F(v) - f_0(x, v))dx\,dv = 0.$$

This condition then yields zero data at infinity for the electric field, and hence a representation for the field results:

$$E(t, x) = \int_{-\infty}^{x} \rho(t, y)dy. \tag{2}$$

Unlike many classical investigations of the Vlasov–Poisson system (see [12] for a complete overview), which assume compact support of the particle distributions, we are interested in studying how the negative ions move to balance the fixed positive background. Hence, we seek solutions $f(t, x, v)$ which tend to $F(v)$ as $|x|\to\infty$ for any t, rather than those which possess compact support or tend to zero as $|x|\to\infty$. Hence, we will assume that $f_0 \in C^1(\mathbb{R}^2)$ is nonnegative with compact support in v, and there is $R>0$ such that for $|x|>R$,

$$f_0(x, v) = F(v) \tag{3}$$

where $F \in C_c^1(\mathbb{R})$ is a nonnegative function. Notice that there is no assumption of compact spatial support on f_0. The introduction of the fixed background implies that $f(t, \cdot, \cdot) \notin L^1(\mathbb{R}^2)$, whence the total positive charge, negative charge, and energy are all infinite.

The impetus for investigating a problem like (1) arises from plasma physicists' attempts to study the stability of a two-species neutral plasma in which a perturbation of the distribution of negative ions is introduced from equilibrium and evolves in such a way as to cancel the effects of the prescribed (perhaps Maxwellian) background of positive charge. Though our assumption of compact velocity support precludes Maxwellian backgrounds for F, the domain of the distribution functions must be truncated regardless, and the method can still approximate values of a Maxwellian. As the initial particle density lacks spatial decay, most of the known mathematical theory regarding existence and uniqueness of solutions to the Cauchy problem does not apply. This is in contrast to the case in which $F\equiv 0$ (cf. [6]) or in the consideration of spatially-periodic solutions (cf. [3]). Recently, the author [14,15] has shown the local-in-time well-posedness of classical solutions to (1). Having answered this question, a next logical step is to construct numerical methods that can determine the behavior of solutions, and this is the objective of the current work. From a computational standpoint, the introduction of the fixed background presents a challenge of accurately representing the distribution functions on a finite region. Hence, our main goal is to construct a particle-in-cell method that can both approximate solutions and generate a region of the computational domain on which these approximations are guaranteed to be accurate. Furthermore, upon testing the method we will utilize it in order to gain some information regarding the long time behavior of solutions.

For problems which incorporate a kinetic description of plasma dynamics, particle methods are often utilized to approximate solutions and tend to be much more efficient than traditional computational techniques for PDEs, such as finite volume or finite element methods. That being said, a good deal of study has been devoted to the development of finite volume schemes for the study of the Vlasov equation (cf. [10,11]). Additionally, hybrid methods which combine aspects of both an Eulerian and Lagrangian framework have been developed, notably in [1,5,16]. As the focus of the current work is on particle methods, however, we must also mention the large collection of studies devoted to different aspects of these approximation techniques, including their construction and implementation [2,7,9,13], and their analysis and convergence [8,4,17,18].

The general structure of a particle method can be described quite simply [2]. As in other numerical methods, phase space (which is (x, v) for kinetic equations) is discretized into grids of finite length. Particles are then initialized with starting positions and velocities at time $t=0$. The charge (and if necessary, current) density is calculated from these particles, and the electric (and if necessary, magnetic) field is calculated from the density. Finally, we compute the force exerted by the field and "move" the particles by changing their respective positions and velocities accordingly. Since the trajectories have now been calculated for the next time step, the process repeats until a stopping time $t=T$ is reached. Weighting schemes often play a large role because particle charges, positions, and velocities must be recorded "at the particles", whereas densities, fields, and forces are indexed by prescribed gridpoints, with the number of particles and gridpoints differing dramatically.

Typically, such a method tracks the evolution of a finite amount of charge within finite spatial and velocity domains. For any simulation of (1), however, the standard truncation of phase space will result in a loss of information as the

particle distributions, which possess non-zero behavior as $|x| \to \infty$, cannot be completely represented. Hence, any method that truncates the spatial domain must continue to track particles that may exit this region and consider the effects of particles originating from outside this region. In the present context, our method will allow particles to move neither into nor out of the computational domain. In order to capture the effects of those particles which may escape, we enlarge the spatial domain at every timestep. Though the positive and negative charges initially cancel outside of $[-R, R]$, both ionic species do exist outside of this interval and may influence the computations as time progresses. Hence, in addition to enlarging the spatial grid, we compute the domain of validity, in which the particles beginning inside the computational domain could not have been influenced by those which began outside. The observed values of ρ and E are only considered valid inside this region of space-time. In the next section, we fully describe our computational method, making these ideas more precise.

2. Description of the method

Though the general structure of a particle method is well-known, we will now construct our specific algorithm to fix notation and, later, discuss results. We begin by truncating the spatial and velocity domains. First, choose $L > 0$ and initially perform the computations on the interval $-L \leq x \leq L$. The assumption on the data is then reformulated to lie within the initial spatial domain, i.e. $R < L$. This ensures that the charges cancel outside of $[-R, R]$ but within $[-L, L]$. Similarly, the velocity domain must be truncated. We choose $Q > 0$ so that particles in the simulation may take on velocities only in the interval $-Q \leq v \leq Q$ at the initial time. Next, we choose $\Delta x, \Delta v > 0$. Using these grid spacings, we create a mesh in phase space by defining

$$x_i = i \cdot \Delta x, \quad i = 1, \ldots, N$$
$$v_j = j \cdot \Delta v, \quad j = 1, \ldots, M$$

where $N, M \in \mathbb{N}$ satisfy $N\Delta x = L$ and $M\Delta v = Q$. Define for every spatial and momentum index $i = 1, \ldots, N$ and $j = 1, \ldots, M$

$$X_{ij}(0) = x_i$$

$$V_{ij}(0) = v_j$$

$$q_{ij} = f_0(X_{ij}(0), V_{ij}(0)) \cdot \Delta x \Delta v.$$

These quantities represent the initial particle positions and velocities, as well as the total negative charge included in the simulation. Here, we have chosen to initially place one representative particle at each gridpoint in phase space, indexed by i, j. Thus, the total number of representative particles included in the simulation is $N \cdot M$. At every timestep of the simulation a leap-frog scheme is utilized for the particle trajectories and first-order averaging methods are used to interpolate the field and charge density values. The functions $X_{ij}(t)$ and $V_{ij}(t)$ will be defined later for $t > 0$. Once they are known, the approximation of the continuous number density is then given by

$$f(t, x, v) = \sum\nolimits_{i,j} q_{ij} \hat{\delta}(x - X_{ij}(t)) \delta(v - V_{ij}(t)) \tag{4}$$

where δ is the Dirac mass and $\hat{\delta}$ is the first-order weighting function defined by

$$\hat{\delta}(x) = \begin{cases} \dfrac{1}{\Delta x}\left(1 - \dfrac{|x|}{\Delta x}\right), & \text{if } |x| < \Delta x \\ 0, & \text{otherwise.} \end{cases}$$

Choose $\Delta t > 0$ and $T > 0$ to represent the time step and stopping time, respectively, and define $t^n = n \cdot \Delta t$ for $n \in \mathbb{N}$. We will write

$$E_i^n = E(t^n, x_i)$$

for field values at the nth timestep and ith gridpoint and define the function $E^n(x)$ by linear interpolation of the gridpoint values E_i^n.

To initiate the leap-frog scheme, we first shift the particle velocities backward by a half timestep using the initial field values. Hence, let

$$V_{ij}(t^{-1/2}) = V_{ij}(0) + E^0(X_{ij}(0)) \cdot \frac{\Delta t}{2}.$$

Now, for $n \in \mathbb{N} \cup \{0\}$, assuming $V_{ij}(t^{n-1/2})$ has been computed, define

$$S^n := \max_{i,j} \left| V_{ij}(t^{n-1/2}) \right|$$

to be the largest velocity at time $t^{n-1/2}$. As the process continues, the velocity domain must be enlarged to allow particles to move as dictated by their interaction with the self-consistent electric field. The compact velocity support of f and F ensure that the largest particle velocity attained at any timestep is finite. Hence, at every timestep S^n is computed and used to extend the spatial boundary of the particle dynamics, which is also enlarged with time to ensure that particles cannot escape. Since the electric field is uniformly bounded [14], we are guaranteed that S^n grows no faster than linearly in time, and this allows us to utilize the finite speed of propagation and localize the computations. Similar procedures have been incorporated into other particle methods for the analogous finite charge problem (for instance, see [4]). To enlarge the length of the spatial domain, we define the increasing sequence L^n by $L^0 = L$ and for every $n \in \mathbb{N}$,

$$L^n := L^{n-1} + S^n \cdot \Delta t.$$

Thus, L^n will be the length of the spatial grid at the nth time step. This will enable the program to continually account for particles which began inside the initial spatial domain, but due to an increase in their velocity would normally move outside of this region. By enlarging the spatial domain at every time step in this fashion, we are able to track such particles and their resulting effects on the induced field.

Assume for $n \in \mathbb{N}$, the characteristics $X_{ij}(t^n)$ and $V_{ij}(t^{n-1/2})$ are known for all $i = 1, \ldots, N$ and $j = 1, \ldots, M$, and that E_i^n is known for $|i| \leq L^n/\Delta x$. For $|i| > L^n/\Delta x$, in light of the neutrality of the plasma, we find $E_i^n = 0$. After a linear interpolation of the field values at gridpoints to generate $E^n(x)$ from E_i^n, define $V_{ij}(t^{n+1/2})$ and $X_{ij}(t^{n+1})$ by

$$\frac{V_{ij}(t^{n+1/2}) - V_{ij}(t^{n-1/2})}{\Delta t} = -E^n(X_{ij}(t^n))$$

$$X_{ij}(t^{n+1}) = X_{ij}(t^n) + \Delta t \cdot V_{ij}(t^{n+1/2}).$$

Next, we describe how to advance the electric field. Define for $i = 1, \ldots, N$ and $n \in \mathbb{N}$,

$$\rho_i^{n+1} = \int (F(v) - f(t^{n+1}, x_i, v)) dv,$$

and by linear interpolation of ρ_i^{n+1}, define $\rho^{n+1}(x)$. Then, let

$$E_i^{n+1} = \int_{-L^{n+1}}^{x_i} \rho^{n+1}(y) dy$$

In practice, this integral is evaluated using the Trapezoidal Rule. The process then continues by advancing the particle positions and velocities, X_{ij} and V_{ij}, to the next time step, t^{n+1}.

Finally, as the process continues, we must determine the region on which our approximations are valid. Since it was necessary to truncate the spatial domain, we were forced to neglect the effects of particles which begin outside of the computational domain and move with large enough velocity to enter it at some time step. This is the essential difficulty created by the infinite mass problem. The new remedy we introduce to combat this problem is to discount the approximations within the region in which these particles could have entered and affected the computations. More specifically, we define for every $n \in \mathbb{N}$,

$$P^n := \sum_{k=0}^{n} S^k$$

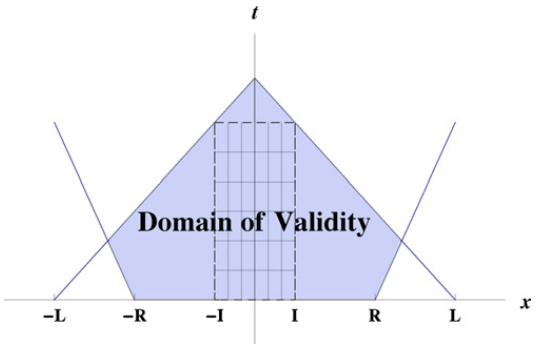

Fig. 1. The domain of validity (shaded) and the chosen long-time region (dashed) for the particle method approximations.

to be the total sum of largest particle velocities up to time $t^{n+1/2}$. Notice that particle velocities are bounded for any fixed time due to the compact v-support of f and F. Since no particle beginning outside the original spatial domain could move with velocity greater than P^n, we may conclude that the portion of the original spatial domain that is unaffected by such particles at any time step t^n lies inside the interval $[-L+P^n\Delta t, L-P^n\Delta t]$. As Fig. 1 illustrates, this provides us with a specific space-time domain on which our numerical approximations are valid.

3. Validation and steady states

In addition to the trivial situation in which $f_0(x, v) = F(v)$ and hence $E \equiv 0$, the previously described particle method was tested using a steady state solution defined as follows. Let

$$f(x, v) = \mathcal{F}\left(\frac{1}{2}|v|^2 + U(x)\right),$$

where

$$\mathcal{F}(e) = \begin{cases} -e & \text{if} \quad e \leq 0 \\ 0 & \text{if} \quad e \geq 0 \end{cases}$$

and

$$U(x) := -\frac{1}{2}(1-x^2)^3\chi_{(-1,1)}(x).$$

From the steady potential $U(x)$, the resulting time-independent field is calculated by

$$\mathcal{E}(x) := U\prime(x) = 3x(1-x^2)^2\chi_{(-1,1)}(x).$$

Additionally, the steady charge density can be found by the derivative of the field

$$\rho(x) = \mathcal{E}\prime(x) = 3(1-x^2)(1-5x^2)\chi_{(-1,1)}(x).$$

Therefore, the distribution of positive charge is determined by ρ and f as

$$\int F(x, v)dv = \rho(x) + \int f(x, v)dv$$

whence we find

$$F(x, v) = \left(3(1-x^2)(1-5x^2) + \frac{2}{3}(1-x^2)^{\frac{9}{2}}\right)\chi_{(-1,1)}(x)\delta(v).$$

Using these functions, the method was implemented for several choices of Δx, Δv, and Δt in order to assure convergence to the correct steady state solution. Table 1 summarizes the results of these runs, listing the error found by calculating the difference between the known steady field solution and the computed electric field at every time step. Additionally, Fig. 2 displays graphs of the exact and approximate steady field values. We expect that as the mesh is refined (and the values of Δt, Δx, and Δv decrease), the error should also decrease for each time. Evaluating the error

Table 1
Error of the field for the steady state solution. Here E_i^n is the computed electric field and $\mathcal{E}_i = \mathcal{E}(x_i)$ is the exact solution evaluated at spatial gridpoints. These values are identical over a minimum of 1000 timesteps for a grid of length $L = 1$.

$\Delta t = \Delta x = \Delta v$	$\sup_i \lvert E_i^n - \mathcal{E}_i \rvert$	$\sup_i \lvert E_i^n \rvert$
0.04	3.20×10^{-3}	0.858
0.02	7.99×10^{-4}	0.858
0.01	2.01×10^{-4}	0.858

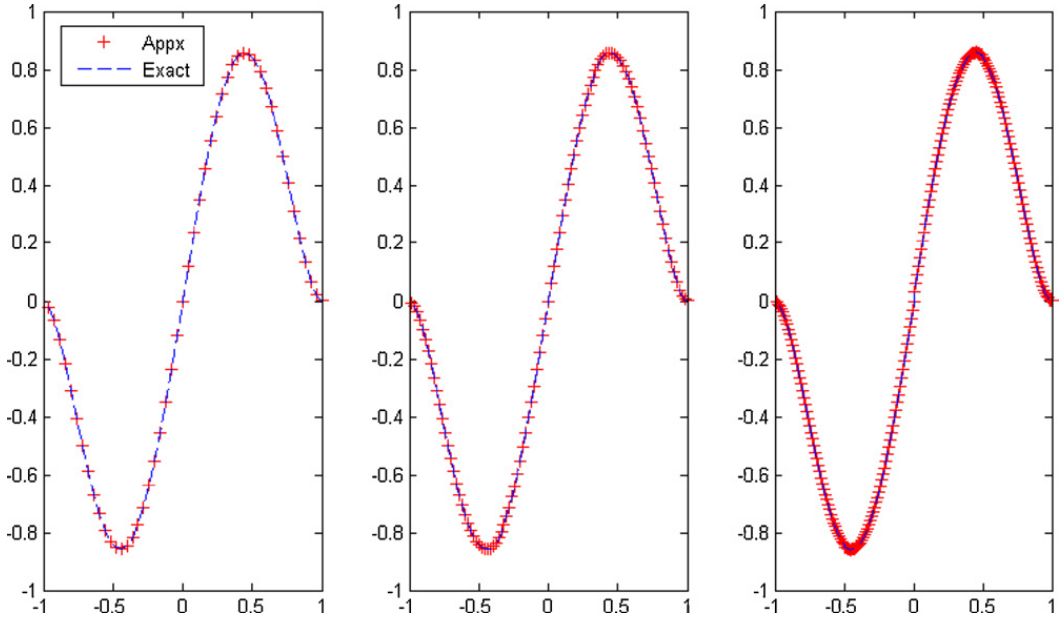

Fig. 2. The steady state electric field for $\Delta x = 0.04$ (left), $\Delta x = 0.02$ (center), and $\Delta x = 0.01$ (right).

values in Table 1, we see that this is the case, and that as the values of all spacings (Δt, Δx, and Δv) are halved, the error decreases by a factor of 4. Thus, we trust the method converges at a suitable rate – approximately first-order in space and second-order in time.

4. Simulation and time asymptotics

Now that the method has been validated for a non-trivial steady state we wish to use it in order to gain information about solutions to (1). More specifically, we will estimate the rate of time decay of the electric field. Consider the following choices for F and f_0. Let $U : \mathbb{R}^2 \times [0, \infty) \to \mathbb{R}$ be defined by

$$U(z, A, B) := A(B - z^2)^3 \chi_{(-\sqrt{B}, \sqrt{B})}(z),$$

and then define

$$F(v) = U(v, 1, 1)$$

and

$$f_0(x, v) = F(v) + x \cdot U(x, 1, 1) \cdot U(v, 0.1, 0.6).$$

The previously described method was implemented with this data, and the results of a few simulations are presented on the following pages. We normalize the velocity domain by choosing $Q = 1$. In each simulation it is important to properly balance the choices of T and L. If L is taken too small or T too large, the computations of the field at each gridpoint will be invalid after some small time $T_0 < T$. Thus, we must ensure that the domain of validity contains a sizeable region $[0, T] \times [-I, I]$ for some $I \leq L$ (see Fig. 1). For each of the following simulations, the mesh sizes are taken to be $\Delta t = \Delta x = \Delta v = 0.01$ and $L = 50$ so that the computations are valid over a reasonably long time

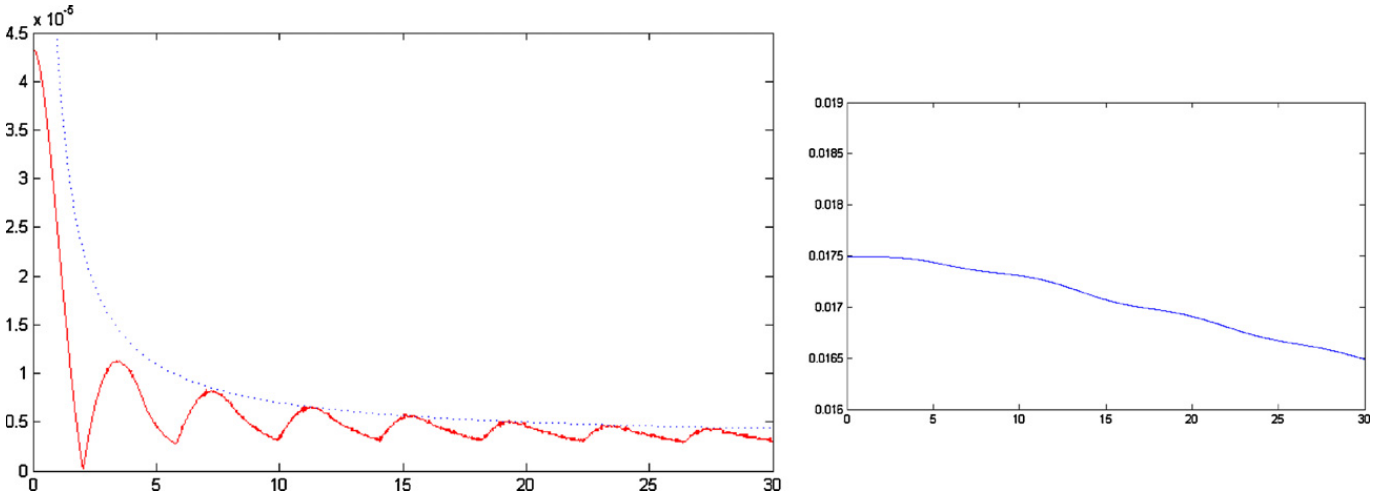

Fig. 3. The maximum of the computed electric field (left, lined), asymptotic behavior (left, dashed), and net energy (right) for $0 \le t \le 30$.

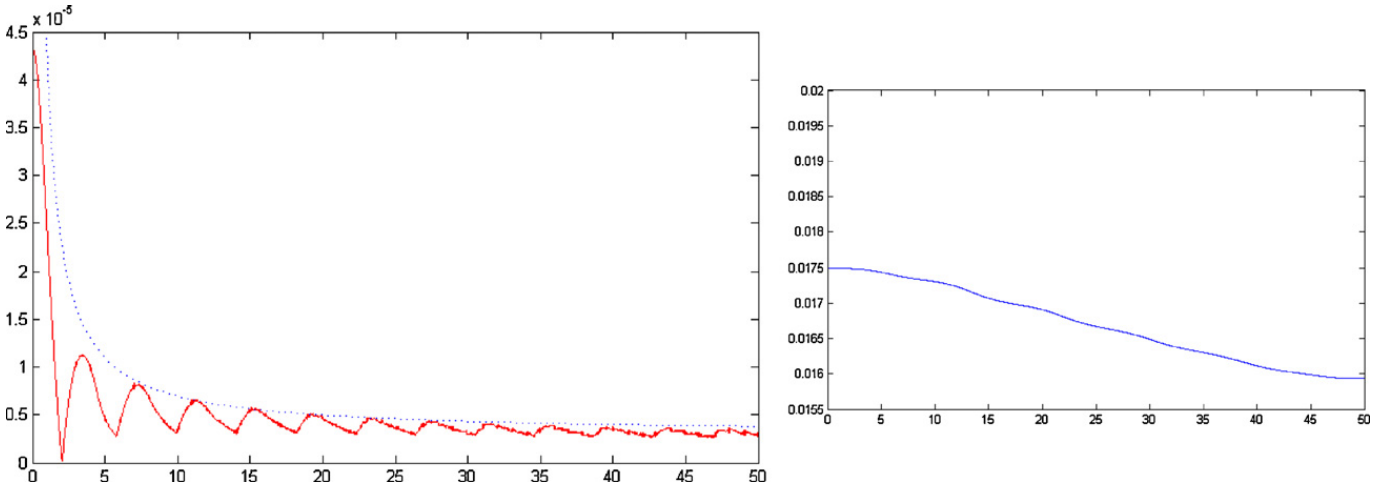

Fig. 4. The maximum value of the computed electric field (left, lined), asymptotic behavior (left, dashed), and net energy (right) for $0 \le t \le 50$.

interval. More specifically, since maximum velocities are on average near $Q = 1$, we expect the time of validity to be approximately $T = L/Q \approx 50$. Fig. 3 displays the computed electric field and conserved energy for $T = 30$, while Fig. 4 in the next section does so for $T = 50$.

From Fig. 3, we can see that the maximum value of the computed electric field is oscillatory, but with decreasing amplitude and mean for $0 \le t \le 30$. In addition, considering the values of t near which the peaks of these oscillations occur, we may conclude this amplitude decreases around a rate of t^{-1} beginning around $t = 7$. This result is demonstrated in Table 2. Specifically, the second row of the table leads us to believe that

$$\sup_i |E(t, x_i)| \approx 1.20 \times 10^{-4} t^{-1}.$$

Hence, the field appears to decay rapidly in the supremum norm, even for simulations performed only up to time $T = 30$. With this, it seems that one cannot expect a general decay rate better than t^{-1} for all solutions.

Table 2
Time rate of decay for the computed electric field.

	$t = 15.6$	$t = 19.2$	$t = 22.8$	$t = 26.0$
$\sup_i \lvert E(t, x_i)\rvert$	7.3×10^{-6}	6.2×10^{-6}	5.2×10^{-6}	4.7×10^{-6}
$\sup_i \lvert E(t, x_i)\rvert \cdot t$	1.14×10^{-4}	1.19×10^{-4}	1.19×10^{-4}	1.22×10^{-4}

To the right of the computed electric field, Fig. 3 shows the net energy in the computational domain for times $0 \leq t \leq 30$. The deviation of the computed energy from its initial value is typically seen as a good measure of the accuracy of the method over time [2]. In this case, the values of the energy range between 1.743×10^{-2}, initially, and 1.654×10^{-2}, near time $T = 30$. The relative change is then calculated as

$$\text{change} = \frac{1.743 \times 10^{-2} - 1.654 \times 10^{-2}}{1.654 \times 10^{-2}} \approx 5.38$$

Thus, we expect our computations to be within 5% and 6% of their actual value. However, as we take larger simulation times, past say $T = 50$, the situation changes and the accuracy of the approximations decreases.

5. Breakdown outside the domain of validity

While the particle method does yield accurate and efficient approximations of (1), limitations do exist within its formulation and implementation. Of course, a limitation of any approximation of a particle distribution without compact support is the truncation of the spatial and velocity domains. One can only simulate domains of finite length, and the previously described particle method will determine the true effects observed, but only within the domain of validity. Hence, the size of this domain is also a limitation. In Fig. 4, we can see that after time $T = 30$, the behavior of the calculated field changes slightly. The decay to zero is impeded and the mean of the oscillation begins to increase. In addition, the figure demonstrates that the energy begins to decrease further away from its initial value after time $T = 30$, as well. Within the simulation, particle velocities have increased, causing the expected domain of validity to shrink. Thus, the computations are only valid up to a time which is strictly less than the stopping time, after which other particles beginning outside of the truncated spatial domain will influence the field behavior within. This displays the limitation of our localized particle method, graphically represented in the previous section by Fig. 1. Computations will inevitably fail to be accurate on any portion of the spatial domain after some time. The only remedy within this context is to enlarge the initial spatial domain, say to $L = 100$ instead of $L = 50$, resulting in more expensive computations.

6. Conclusions

In the present study, a particle method was constructed, validated, and implemented to approximate solutions of (1) which do not possess compact support. Instead, such solutions tend to a fixed background of charge as $|x| \to \infty$ and thus lead to infinite positive and negative charge in the plasma. Computationally, this presents a few challenges as the support of the distribution of ions and electrons cannot be effectively truncated without the loss of information. This was overcome by localizing the method and generating a region in space-time on which the computations remain valid. The numerical method was also used to determine the large time behavior of the electric field. In the future one would like to formulate similar methods to approximate distribution functions with non-compact momentum support, such as a Maxwellian. This would provide a significant challenge as unbounded momenta in the system would preclude the aforementioned localization. Similarly, it would be beneficial to extend this method to higher spatial and momentum dimensions. This would be a seemingly tractable problem since *a priori* velocity bounds are known even in higher dimensions, though the analogous domains of validity would correspond to the intersection of cones in space-time. It is our hope that the future development of such methods will lead to better intuition regarding the behavior of such systems.

Acknowledgements

The author gratefully acknowledges support from National Science Foundation and the United States Naval Academy Research Council. This material is based upon work supported by the NSF under Grant no. DMS-0908413.

References

[1] N. Besse, Convergence of a semi-Lagrangian scheme for the one-dimensional Vlasov–Poisson system, SIAM J. Numer. Anal. 42 (2004) 350–382 (electronic).

[2] C. Birdsall, A. Langdon, Plasma Physics Via Computer Simulation, Institute of Physics, Series in Plasma Physics, Taylor and Francis, New York, NY, 1991.
[3] M. Bostan, Existence and uniqueness of the mild solution for the 1D Vlasov–Poisson initial-boundary value problem, SIAM J. Math. Anal. 37 (2005) 156–188.
[4] M. Bostan, Analysis of a particle method for the one-dimensional Vlasov–Maxwell system, Numer. Methods Partial Differential Equations 25 (2009) 757–782.
[5] C. Cheng, G. Knorr, The integration of the vlasov equation in configuration space, J. Comput. Phys. 22 (1976) 330–351.
[6] J. Cooper, A. Klimas, Boundary value problems for the Vlasov–Maxwell equation in one dimension, J. Math. Anal. Appl. 75 (1980) 306–329.
[7] G.H. Cottet, P.A. Raviart, Particle methods for the one-dimensional Vlasov–Poisson equations, SIAM J. Numer. Anal. 21 (1984) 52–76.
[8] G.H. Cottet, P.A. Raviart, On particle-in-cell methods for the Vlasov–Poisson equations, Transp. Theory Statist. Phys. 15 (1986) 1–31.
[9] P. Degond, F. Deluzet, L. Navoret, An asymptotically stable particle-in-cell (PIC) scheme for collisionless plasma simulations near quasineutrality, C. R. Math. Acad. Sci. Paris 343 (2006) 613–618.
[10] E. Fijalkow, A numerical solution to the Vlasov equation, Comput. Phys. Commun. 116 (1999) 319–328.
[11] F. Filbet, E. Sonnendrücker, P. Bertrand, Conservative numerical schemes for the Vlasov equation, J. Comput. Phys. 172 (2001) 166–187.
[12] R.T. Glassey, The Cauchy Problem in Kinetic Theory, Society for Industrial and Applied Mathematics (SIAM), Philadelphia, PA, 1996.
[13] R. Hockney, J. Eastwood, Computer Simulation using Particles, Institute of Physics, 1988.
[14] S. Pankavich, Local existence for the one-dimensional Vlasov–Poisson system with infinite mass, Math. Methods Appl. Sci. 30 (2007) 529–548.
[15] S. Pankavich, Explicit solutions of the one-dimensional Vlasov–Poisson system with infinite mass, Math. Methods Appl. Sci. 31 (2008) 375–389.
[16] E. Sonnendrücker, J. Roche, P. Bertrand, A. Ghizzo, The semi-Lagrangian method for the numerical resolution of the Vlasov equation, J. Comput. Phys. 149 (1999) 201–220.
[17] H.D. Victory Jr., G. Tucker, K. Ganguly, The convergence analysis of fully discretized particle methods for solving Vlasov–Poisson systems, SIAM J. Numer. Anal. 28 (1991) 955–989.
[18] S. Wollman, Convergence of a numerical approximation to the one-dimensional Vlasov–Poisson system, Transp. Theory Statist. Phys. 19 (1990) 545–562.